J|A|C|S
COMMUNICATIONS

Published on Web 12/15/2006

Regioselective Arene Hydroxylation Mediated by a (μ-Peroxo)diiron(III) Complex: A Functional Model for Toluene Monooxygenase

Mai Yamashita,[†] Hideki Furutachi,[†] Takehiko Tosha,[‡] Shuhei Fujinami,[†] Wataru Saito,[†] Yonezo Maeda,[#] Kenji Takahashi,[†] Koji Tanaka,[§] Teizo Kitagawa,[‡] and Masatatsu Suzuki*[,†]

Division of Material Sciences, Graduate School of Natural Science and Technology, Kanazawa University, Kakuma-machi, Kanazawa 920-1192, Japan, Okazaki Institute for Integrative Bioscience and Okazaki Institute for Molecular Science, National Institutes of Natural Sciences, Myodaiji, Okazaki, 444-8585, Japan, and Department of Chemistry, Graduate School of Sciences, Kyushu University, 6-10-1 Hakozaki, Higashi-ku, Fukuoka 812-8581, Japan

Received June 6, 2006; E-mail: suzuki@cacheibm.s.kanazawa-u.ac.jp

The diiron center of toluene monooxygenase hydroxylase (TMOH) is capable of oxidizing arenes, alkenes, and haloalkanes.[1] Recently, the diiron center of toluene/*o*-xylene monooxygenase hydroxylase (ToMOH) has been shown to have a carboxylate-rich environment similar to that of soluble methane monooxygenase (MMOH).[1a,2] Extensive studies of MMOH have provided a fundamental basis for the understanding of the structural and spectroscopic properties and the reaction mechanisms. In the catalytic process of MMOH, peroxodiiron(III) and bis(μ-oxo)diiron(IV) intermediates have been detected, the latter of which is responsible for hydroxylation of methane.[2,3] In addition, a peroxo-intermediate has been shown to be capable of the epoxidation of alkenes.[4] Very recently, two intermediates, a peroxodiiron(III) form and a diiron(III, IV) form having a W• radical, have been discovered in I100W ToMOH mutant.[5] Another type of diiron center having a histidine-rich environment has also been proposed for alkane ω-hydroxylase (AlkB),[6] suggesting the diversity of the coordination environments of the diiron centers in the dioxygen activating enzymes.

Some synthetic TMOH model complexes have been reported, which hydroxylate phenyl group of the supporting ligand in the reactions with oxidants such as H_2O_2, *m*-CPBA, and O_2.[7] However, no intermediate has been observed in the hydroxylation process. Herein, we report two types of peroxodiiron(III) complexes, $[Fe_2(L^{Ph4})(RCO_2)(O_2)]^{2+}$ (R = Ph_3C (oxy-**1**) and Ph (oxy-**2**)) generated in the reaction of diiron(II) complexes $[Fe_2(L^{Ph4})(RCO_2)]^{2+}$ (R = Ph_3C (**1**) and Ph (**2**)) with O_2; the former leads to regioselective hydroxylation of a phenyl group of L^{Ph4} and the latter exhibits reversible deoxygenation (L^{Ph4} = *N*,*N*,*N*′,*N*′-tetrakis[(1-methyl-2-phenyl-4-imidazolyl)methyl]-1,3-diamino-2-propanolate). The reactions mimic TMOH and hemerythrin (Hr) reactivity, respectively. They provide further insights into the reactivity of the peroxodiiron(III) complexes having a nitrogen-rich coordination environment like AlkB and Hr.

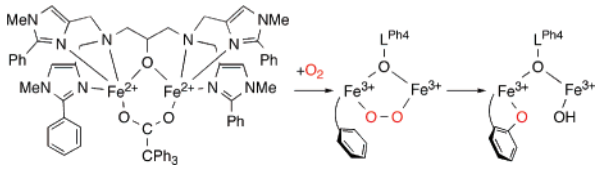

Crystal structures of **1** and **2** revealed that they are pentacoordinate, and two irons are bridged by alkoxide of L^{Ph4} and an exogenous carboxylate (Figure S1, Supporting Information).[8] They reacted with O_2 to generate dark-green oxy-**1** (ESI-MS: *m*/*z* 600.2 and 602.2 for $^{18}O_2$ sample) and oxy-**2** (ESI-MS exhibited only signals corresponding to **2** (*m*/*z* 501.2)) in CH_2Cl_2 at −40 °C. The electronic spectra showed absorption bands at 665 nm (∼2300 M^{-1} cm^{-1}) for oxy-**1** and ∼710 nm (∼1500 M^{-1} cm^{-1}) for oxy-**2** (Figure S4) assignable to the CT transitions from O_2^{2-} to Fe(III) center (LMCT). The absorption band of oxy-**2** is very broad compared to that of oxy-**1**, suggesting some electronic and/or structural change(s) in those complexes. Mössbauer spectra of powdery samples of oxy-**1**·BPh_4 and oxy-**2**·BPh_4 at 80 K showed a quadrupole doublet with δ (ΔE_Q) = 0.57 (1.44) and 0.58 (1.17) mm s^{-1}, respectively (Figures S6 and S7), which are in the range of those of the peroxodiiron(III) complexes.[9,10]

Both oxy-species are stable at −40 °C for several days. Oxy-**2** is reversibly deoxygenated by bubbling N_2 and warming a solution up to room temperature (Figure S4B). In contrast, oxy-**1** did not show reversible deoxygenation; warming a solution up to 25 °C with bubbling of N_2 generated a dark-blue solution (vide infra).

Resonance Raman spectra of oxy-**1** and oxy-**2** showed isotope sensitive bands at 873 cm^{-1} ($^{16-18}\Delta$ = 50 cm^{-1}) and 480 cm^{-1} (16 cm^{-1}) and at 840 cm^{-1} ($^{16-18}\Delta$ = 45 cm^{-1}) and 459 cm^{-1} (20 cm^{-1}), respectively (Figure 1). The bands at 873 and 840 cm^{-1} can be assigned to the ν(O−O) vibrations, and the bands at 480 and 459 cm^{-1} can be assigned to the ν_s(Fe−O_{O-O}) vibrations. It is noted that there is a significant difference in both ν(O−O) and ν_s(Fe−O_{O-O}) frequencies between these two complexes. The ν(O−O) and ν_s(Fe−O_{O-O}) have been shown to depend on the Fe−O−O angle; as the Fe−O−O angle becomes larger, the ν(O−O) becomes higher and the ν_s(Fe−O_{O-O}) lower by mechanical coupling.[11] This is not the case for those of the present complexes. It has also been shown that the LMCT transition energy and the ν(O−O) and ν_s(Fe−O_{O-O}) frequencies of the peroxodiiron(III) complexes can be good probes for elucidation of the bonding nature of the Fe−O_{O-O} and Lewis acidity of Fe(III) center.[2d,10,12] The high ν(O−O) and ν_s(Fe−O_{O-O}) frequencies of oxy-**1** relative to those of oxy-**2** suggest a stronger Fe−O_{O-O} bonding owing to stronger σ and π donation from the peroxo ligand, which decreases the electron densities of the π* orbitals of the peroxo ligand. This is in line with a blue shift of the LMCT transition energy of oxy-**1** relative to that of oxy-**2**. Furthermore, this effect seems to be responsible for the high dioxygen affinity of oxy-**1** relative to that of oxy-**2** (vide infra). However, the origin of such a significant difference between these two complexes remains unclear.

Complex **2** did not produce measurable oxy-**2** in CH_2Cl_2 at 25 °C under O_2, whereas irreversible oxidation occurred for several hours to give a brown species. In contrast, **1** is oxygenated under O_2 at 25 °C to give oxy-**1**, which is not stable and decomposes to generate a dark-blue species (a red line in Figure 2). The crystal structure of this species ($[Fe_2(L^{Ph4}\text{-}O)(Ph_3CCO_2)(OH)](ClO_4)_2$·$3CH_2Cl_2$·$2H_2O$ (**1**-O·ClO_4)) revealed that one of the phenyl groups of L^{Ph4} is regio-

[†] Kanazawa University.
[‡] Okazaki Institute for Integrative Bioscience.
[§] Okazaki Institute for Molecular Science.
[#] Kyushu University.

10.1021/ja063987z CCC: $37.00

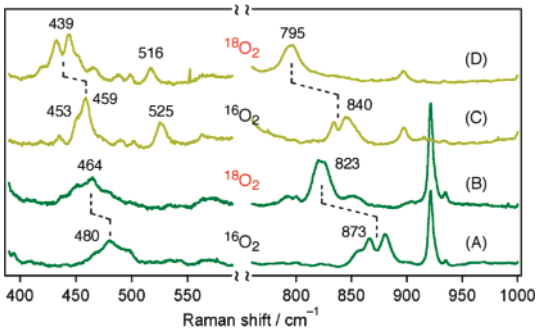

Figure 1. Resonance Raman spectra of oxy-**1** prepared from (A) $^{16}O_2$ and (B) $^{18}O_2$ in CH_2Cl_2/CH_3CN (1:1) at −80 °C and oxy-**2** prepared from (C) $^{16}O_2$ and (D) $^{18}O_2$ in CH_2Cl_2 at −80 °C (607 nm laser excitation).

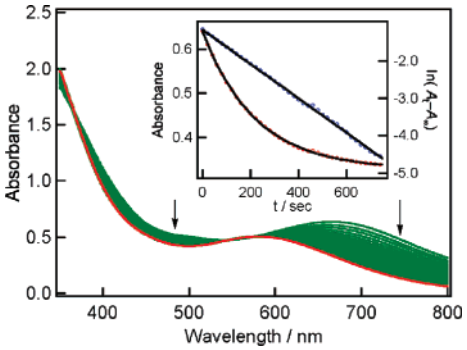

Figure 2. Electronic spectral change of oxy-**1** (0.358 mM) in CH_2Cl_2 at 25 °C under O_2 (20 s interval). Inset is a first-order kinetic plot for the conversion to **1**-O (668 nm trace).

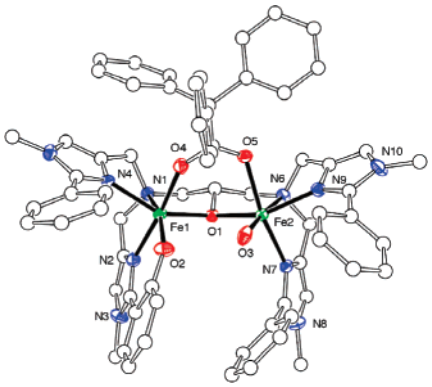

Figure 3. ORTEP view (50% probability) of **1**-O cation. Selected bond distances (Å) and angle (deg): Fe1−O1, 2.008(4); Fe1−O2, 1.881(4); Fe1−O4, 2.063(4); Fe1−N1, 2.294(4); Fe1−N2, 2.075(4); Fe1−N4, 2.130(4); Fe2−O1, 2.051(3); Fe2−O3, 1.863(4); Fe2−O5, 2.108(4); Fe2−N6, 2.279(4); Fe2−N7, 2.122(4); Fe2−N9, 2.139(5); Fe1−O1−Fe2, 119.6(2).

selectively hydroxylated as shown in Figure 3. Conversion from oxy-**1** to **1**-O in CH_2Cl_2 under O_2 at 25 °C was also confirmed by ESI-MS and Mössbauer spectroscopies (Figures S5 and S6).[13] A ligand-recovery experiment after decomposition at 25 °C revealed that the hydroxylation yield is ∼90%. An isotope labeling experiment using $^{18}O_2$ showed that the oxygen of L^{Ph4}-O comes from dioxygen (Figure S9).

Kinetic study revealed that the hydroxylation obeys first-order kinetics (see Supporting Information). Activation parameters are $\Delta H^{\ddagger} = 70$ kJ mol^{-1} and $\Delta S^{\ddagger} = -55$ J K^{-1} mol^{-1}, indicating that the hydroxylation mediated by oxy-**1** is enthalpically and entropically unfavorable compared to those reported for some (μ-η^2:η^2-peroxo)dicopper(II) complexes with a dinucleating ligand having a *m*-xylyl linker ($\Delta H^{\ddagger} = 50$ kJ mol^{-1}, $\Delta S^{\ddagger} = -35$ J K^{-1} mol^{-1} and $\Delta H^{\ddagger} = 63$ kJ mol^{-1}, $\Delta S^{\ddagger} = -11$ J K^{-1} mol^{-1}).[14]

In summary, we have succeeded in the synthesis of peroxodiiron(III) complexes which have two faces modulated by the stereochemistry of bridging carboxylates: oxy-**1** having $Ph_3CCO_2^-$ causes arene hydroxylation of the supporting ligand L^{Ph4} which mimics the function of TMOH, whereas oxy-**2** having $PhCO_2^-$ exhibits reversible deoxygenation like Hr. For a fuller understanding of such a remarkable change in reactivity, structural information of the oxy-species is needed.

Acknowledgment. Financial support by Grant-in-Aid for Scientific Research from the Ministry of Education, Culture, Sports, Science and Technology, Japan (H.F., T.K., and M.S.) is acknowledged.

Supporting Information Available: Details of syntheses, characterization of the complexes, X-ray crystallography, kinetics, and ligand recovery experiment. This material is available free of charge via the Internet at http://pubs.acs.org.

References

(1) (a) Sazinsky, M. H.; Bard, J.; Donato, A. D.; Lippard, S. J. *J. Biol. Chem.* **2004**, *279*, 30600−30610. (b) Mitchell, K. H.; Rogge, C. E.; Gierahn, T.; Fox, B. G. *Proc. Natl. Acad. Sci. U.S.A.* **2003**, *100*, 3784−3789. (c) Mitchell, K. H.; Studts, J. M.; Fox, B. G. *Biochemistry* **2002**, *41*, 3176−3188. (d) Moe, L. A.; Hu, Z.; Deng, D.; Austin, R. N.; Groves, J. T.; Fox, B. G. *Biochemistry* **2004**, *43*, 15688−15701.

(2) For example, see: (a) Sazinsky, M. H.; Lippard, S. J. *Acc. Chem. Res.* **2006**, *39*, 558−566. (b) Baik, M.-H.; Newcomb, M.; Friesner, R. A.; Lippard, S. J. *Chem. Rev.* **2003**, *103*, 2385−2419. (c) Merkx, M.; Kopp, D. A.; Sazinsky, M. H.; Blazyk, J. L.; Müller, J.; Lippard, S. J. *Angew. Chem., Int. Ed.* **2001**, *40*, 2782−2807. (d) Solomon, E. I.; Brunold, T. C.; Davis, M. I.; Kemsley, J. N.; Lee, S.-K.; Lehnert, N.; Neese, F.; Skulan, A. J.; Yang, Y.-S.; Zhou, J. *Chem. Rev.* **2000**, *100*, 235−349. (e) Wallar, B. J.; Lipscomb, J. D. *Chem. Rev.* **1996**, *96*, 2625−2657.

(3) (a) Liu, K. E.; Wang, D.; Huynh, B. H.; Edmondson, D. E.; Salifoglou, A.; Lippard, S. J. *J. Am. Chem. Soc.* **1994**, *116*, 7465−7466. (b) Liu, K. E.; Valentine, A. M.; Wang, D.; Huynh, B. H.; Edmondson, D. E.; Salifoglou, A.; Lippard, S. J. *J. Am. Chem. Soc.* **1995**, *117*, 10174−10185. (c) Lee, S.-K.; Fox, B. G.; Froland, W. A.; Lipscomb, J. D.; Münck, E. *J. Am. Chem. Soc.* **1993**, *115*, 6450−6451. (d) Shu, L. J.; Nesheim, J. C.; Kauffmann, K.; Münck, E.; Lipscomb, J. D.; Que, L., Jr. *Science* **1997**, *275*, 515−518.

(4) Valentine, A. M.; Stahl, S. S.; Lippard, S. J. *J. Am. Chem. Soc.* **1999**, *121*, 3876−3887.

(5) Murray, L. J.; García-Serres, R.; Naik, S.; Huynh, B. H.; Lippard, S. J. *J. Am. Chem. Soc.* **2006**, *128*, 7458−7459.

(6) (a) Shanklin, J.; Achim, C.; Schmidt, H.; Fox, B. G.; Münck, E. *Proc. Natl. Acad. Sci. U.S.A.* **1997**, *94*, 2981−2986. (b) Groves, J. T. *J. Inorg. Biochem.* **2006**, *100*, 434−447.

(7) (a) Ménage, S.; Galey, J.-B.; Dumats, J.; Hussler, G.; Seité, M.; Luneau, I. G.; Chottard, G.; Fontecave, M. *J. Am. Chem. Soc.* **1998**, *120*, 13370−13382. (b) Furutachi, H.; Murayama, M.; Shiohara, A.; Yamazaki, S.; Fujinami, S.; Uehara, A.; Suzuki, M.; Ogo, S.; Watanabe, Y.; Maeda, Y. *Chem. Commun.* **2003**, 1900−1901. (c) Avenier, F.; Dubois, L.; Latour, J.-M. *New J. Chem.* **2004**, *28*, 782−784.

(8) Syntheses, X-ray crystallography, spectroscopic characterization, ligand recovery experiments, and kinetics are given in Supporting Information.

(9) (a) Suzuki, M.; Furutachi, H.; Okawa, H. *Coord. Chem. Rev.* **2000**, *200−202*, 105−129. (b) Tshuva, E. Y.; Lippard S. *J. Chem. Rev.* **2004**, *104*, 987−1012.

(10) Zhang, X.; Furutachi, H.; Fujinami, S.; Nagatomo, S.; Maeda, Y.; Watanabe, Y.; Kitagawa, T.; Suzuki, M. *J. Am. Chem. Soc.* **2005**, *127*, 826−827.

(11) Brunold, T. C.; Tamura, N.; Kitajima, N.; Moro-oka, Y.; Solomon, E. I. *J. Am. Chem. Soc.* **1998**, *120*, 5674−5690.

(12) Skulan, A. J.; Brunold, T. C.; Baldwin, J.; Saleh, L.; Bollinger, J. M., Jr.; Solomon, E. I. *J. Am. Chem. Soc.* **2004**, *126*, 8842−8855.

(13) ESI-MS showed successive conversion from oxy-**1** (*m/z* 600.2 $\{Fe_2(L^{Ph4})(Ph_3CCO_2)(O_2)\}^{2+}$) to **1**-O (*m/z* 600.2 $\{Fe_2(L^{Ph4}\text{-}O)(Ph_3CCO_2)(OH)\}^{2+}$), the latter of which was identified as $\{Fe_2(L^{Ph4}\text{-}O)(Ph_3CCO_2)(OMe)\}^{2+}$ (*m/z* 607.2) by the addition of MeOH into the reaction solution. Mössbauer spectrum of a powdery sample isolated by rapid-freeze quenching showed the presence of oxy-**1** (δ (ΔE_Q) = 0.57 (1.44) mm s^{-1}) and **1**-O (two sets of quadrupole doublets with equal intensities δ (ΔE_Q) = 0.50 (0.72) and 0.48 (1.63) mm s^{-1}) (see Figures S5 and S6).

(14) (a) Karlin, K. D.; Nasir, M. S.; Cohen, B. I.; Cruse, R. W.; Kaderli, S.; Zuberbühler, A. D. *J. Am. Chem. Soc.* **1994**, *116*, 1324−1336. (b) Matsumoto, T.; Furutachi, H.; Kobino, M.; Tomii, M.; Nagatomo, S.; Tosha, T.; Osako, T.; Fujinami, S.; Itoh, S.; Kitagawa, T.; Suzuki, M. *J. Am. Chem. Soc.* **2006**, *128*, 3874−3875.

JA063987Z